N-Glycosylation affects the stability and barrier function of the MUC16 mucin

Received for publication, November 28, 2016, and in revised form, May 3, 2017 Published, Papers in Press, May 9, 2017, DOI 10.1074/jbc.M116.770123

Takazumi Taniguchi[‡1], Ashley M. Woodward[‡1], Paula Magnelli[§], Nicole M. McColgan[‡], Sylvain Lehoux[¶], Sarah Melissa P. Jacobo[‡], Jérôme Mauris[‡], and Pablo Argüeso[‡2]

From the [‡]Schepens Eye Research Institute and Massachusetts Eye and Ear, Department of Ophthalmology, Harvard Medical School, Boston, Massachusetts 02114, [§]New England Biolabs, Ipswich, Massachusetts 01938, and the [¶]Department of Surgery, Beth Israel Deaconess Medical Center, Harvard Medical School, Boston, Massachusetts 02215

Edited by Amanda J. Fosang

Transmembrane mucins are highly *O*-glycosylated glycoproteins that coat the apical glycocalyx on mucosal surfaces and represent the first line of cellular defense against infection and injury. Relatively low levels of *N*-glycans are found on transmembrane mucins, and their structure and function remain poorly characterized. We previously reported that carbohydrate-dependent interactions of transmembrane mucins with galectin-3 contribute to maintenance of the epithelial barrier at the ocular surface. Now, using MALDI-TOF mass spectrometry, we report that transmembrane mucin *N*-glycans in differentiated human corneal epithelial cells contain primarily complex-type structures with *N*-acetyllactosamine, a preferred galectin ligand. In *N*-glycosylation inhibition experiments, we find that treatment with tunicamycin and siRNA-mediated knockdown of the Golgi *N*-acetylglucosaminyltransferase I gene (*MGAT1*) induce partial loss of both total and cell-surface levels of the largest mucin, MUC16, and a concomitant reduction in glycocalyx barrier function. Moreover, we identified a distinct role for *N*-glycans in promoting MUC16's binding affinity toward galectin-3 and in causing retention of the lectin on the epithelial cell surface. Taken together, these studies define a role for *N*-linked oligosaccharides in supporting the stability and function of transmembrane mucins on mucosal surfaces.

Epithelial cells lining mucosal surfaces, such as those of the ocular surface, respiratory, gastrointestinal, and reproductive tracts, perform functions ascribed to maintaining a robust barrier that protects against environmental insult (1, 2). Integral to these functions is the carbohydrate-rich glycocalyx present along apical membranes on epithelial cells. A major component of the epithelial glycocalyx is a group of highly glycosylated, high-molecular-weight glycoproteins termed transmembrane mucins. These can extend between 200 and 500 nm above the plasma membrane and cover the extracellular domain of most membrane glycoproteins, which usually protrude <30 nm (3, 4).

Several transmembrane mucins (MUC1, MUC3A, MUC3B, MUC4, MUC12, MUC13, MUC15, MUC16, MUC17, MUC20, and MUC21) have been identified so far (5). Among them, MUC16 is the largest with 22,152 amino acids and represents the longest human protein after the muscle protein titin. A number of mucosal surfaces express MUC16, such as the ocular surface and the respiratory, gastric, and female reproductive tracts (6). The glycosylation of transmembrane mucins is cell type-specific and has been linked to the selective expression of glycosyltransferases (7). Alteration of transmembrane mucin protein biosynthesis and/or glycosylation is associated with multiple pathologies, such as inflammatory bowel disease, allergy, cancer, and dry eye, a disease affecting >5 million people in the United States alone (6, 8–10).

Structurally, transmembrane mucins contain a single membrane-spanning domain, a cytoplasmic tail, and an extensive extracellular domain composed of a variable number of tandem-repeat sequences. These repetitive sequences are rich in serine and threonine residues covalently modified with *O*-linked glycans and provide clusters of specific carbohydrate moieties crucial to mucin structure and function. The stoichiometric power of these multivalent tandem repeats are known to facilitate specific interactions with glycan-binding proteins and allow control of the local microenvironment (11). The peptide backbone of MUC16 contains a tandem-repeat region with up to 60 repeats, each of which is composed of 156 amino acids (5). Analysis of the carbohydrate content of MUC16 shows that it accounts for up to 77% of its weight, and it is characterized by the presence of high amounts of carbohydrates commonly found in *O*-glycans, such as galactose and galactosamine (12). In contrast, relatively low levels of *N*-glycans are found on transmembrane mucins, and their structure and function remain relatively understudied, particularly in healthy tissue.

The transfer of *N*-glycans to nascent proteins occurs in the lumen of the endoplasmic reticulum and is a critical step affecting the properties of a glycoprotein in terms of structure and biological function. *N*-Glycans ensure proper protein folding before their exit from the endoplasmic reticulum through interaction with lectin-like chaperones; aberrant or impaired

This work was supported by the National Institutes of Health Grants R01EY014847 and R01EY026147 (NEI; to P. A.), NEI Core Grant P30EY003790, and the National Center for Functional Glycomics Grant P41GM103694 (NIGMS; to S. L.). The authors declare that they have no conflicts of interest with the contents of this article. The content is solely the responsibility of the authors and does not necessarily represent the official views of the National Institutes of Health.

This article contains supplemental Table S1.

[1] Both authors contributed equally to this work.

[2] To whom correspondence should be addressed: Schepens Eye Research Institute and Massachusetts Eye and Ear, Department of Ophthalmology, Harvard Medical School, 20 Staniford St., Boston, MA 02114. Tel.: 617-912-0249; E-mail: pablo_argueso@meei.harvard.edu.

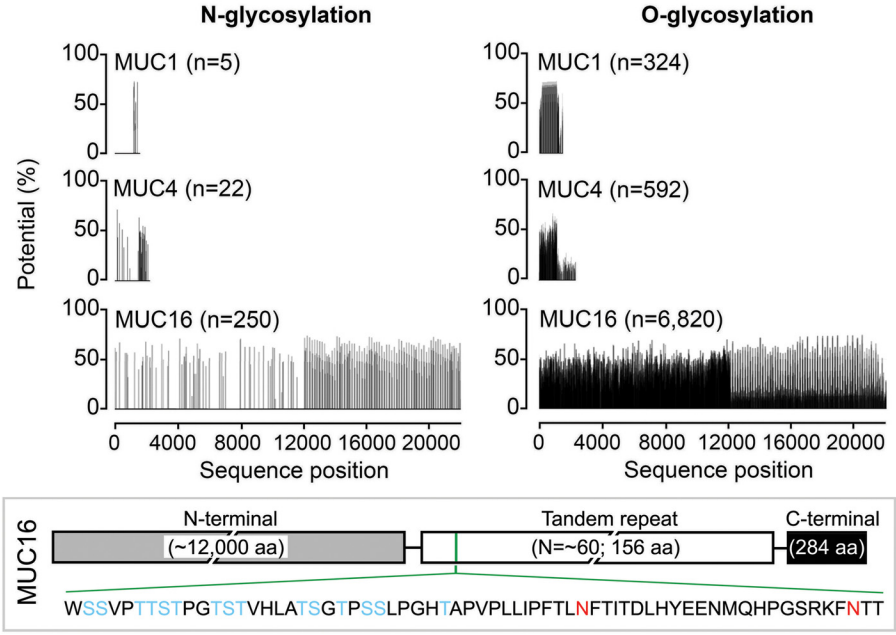

Figure 1. *N*-Glycosylation on transmembrane mucins. Schematic diagram of the total number of putative *N*- and *O*-glycosylation sites on the full-length sequences of human MUC1, MUC4, and MUC16, given as a function of amino acid (*aa*) sequence position. The range of glycosylation potential is shown as a percentage. The putative *N*-glycosylation sites on MUC16 reside predominantly within the C-terminal and tandem-repeat regions. Clustered serine and threonine residues and two conserved asparagine residues within a MUC16 tandem repeat are shown in *blue* and *red*, respectively.

N-glycosylation in the endoplasmic reticulum leads to misfolded or unfolded proteins that are tagged by ubiquitination and then degraded by the proteasome (13). To cope with the stress, cells activate an integrated intracellular signaling pathway to correct the protein-folding defect, collectively called the unfolded protein response. On mature proteins, *N*-glycan number and degree of branching controls the residence time and biological activity of cell-surface receptors by regulating the formation of galectin-glycoprotein lattices (14, 15). The activities of medial Golgi-branching *N*-acetylglucosaminyltransferases are critical in this process, as they initiate the glycosylation events that generate sequences recognized by galectins. Recent reports indicate that transmembrane mucins bind galectins to regulate multiple functions including signal transduction, cell growth and survival, and glycocalyx barrier function (16–19). Whereas *O*-glycosylation and the Thomsen-Friedenreich antigen in particular have been shown to regulate the binding affinity of transmembrane mucins toward galectins, less clear, however, is the contribution of *N*-glycans and the Golgi *N*-glycan branching pathway in this process (20). In the present study we have characterized the *N*-glycans associated with transmembrane mucins isolated from differentiated cultures of human corneal epithelial cells. The analysis demonstrates the presence of complex-type structures with *N*-acetyllactosamine residues. Furthermore, we found that *N*-glycans and the Golgi *N*-glycan branching pathway maintain MUC16 stability and glycocalyx barrier function. Mechanistically, we show that *N*-glycans promote binding affinity of MUC16 toward galectin-3 and cause retention of the lectin on the epithelial cell surface. These data establish a distinct role for *N*-linked oligosaccharides in maintaining the integrity of transmembrane mucins and supporting the protective function of the corneal epithelial glycocalyx.

Results

Mucin N-glycosylation and the N-glycan-branching pathway in ocular surface epithelia

Mucosal cells in both simple and stratified epithelia frequently express various transmembrane mucins on their apical surfaces; for instance, the ocular surface (21), endometrium (22), and the respiratory tract (23) produce MUC1, MUC4, and MUC16. As shown *in silico* using the NetNGlyc 1.0 and NetOGlyc 4.0 servers, the predicted *N*-glycosylation sites on these mucins represent a marginal fraction compared with the *O*-glycosylation sites and tend to concentrate within the C-terminal region of MUC1 and MUC4 and within the C-terminal and tandem-repeat regions of MUC16 (Fig. 1). MUC1 and MUC4 have 5 and 22 predicted *N*-glycosylation sites, respectively, whereas 250 sites are present within the MUC16 sequence, including two reportedly conserved within the tandem-repeat region (24).

Glycosyltransferase expression analysis by qPCR[3] revealed that human corneal and conjunctival epithelial cells at the ocular surface produce transcripts encoding enzymes involved in the formation of *N*-glycan branching structures in the medial Golgi (Fig. 2*a*). These include the *N*-acetylglucosaminyltransferases I, II, IV, and V (MGAT1, MGAT2, MGAT4, and MGAT5) required for the biosynthesis of hybrid and complex *N*-glycans and α-mannosidase II enzymes that modify high mannose *N*-glycan precursors. Comparison of the patterns of gene expression of the enzymes in the stratified cell lines

[3] The abbreviations used are: qPCR, quantitative PCR; BiP, binding immunoglobulin protein; CHOP, CCAAT-enhancer-binding protein homologous protein; ConA, concanavalin A; Hex, hexose; HexNAc, *N*-acetylhexosamine; PAS, periodic acid-Schiff; PNGase F, peptide N-glycosidase F; rhGal-3, recombinant human galectin-3; sXBP1, spliced X-box binding protein 1.

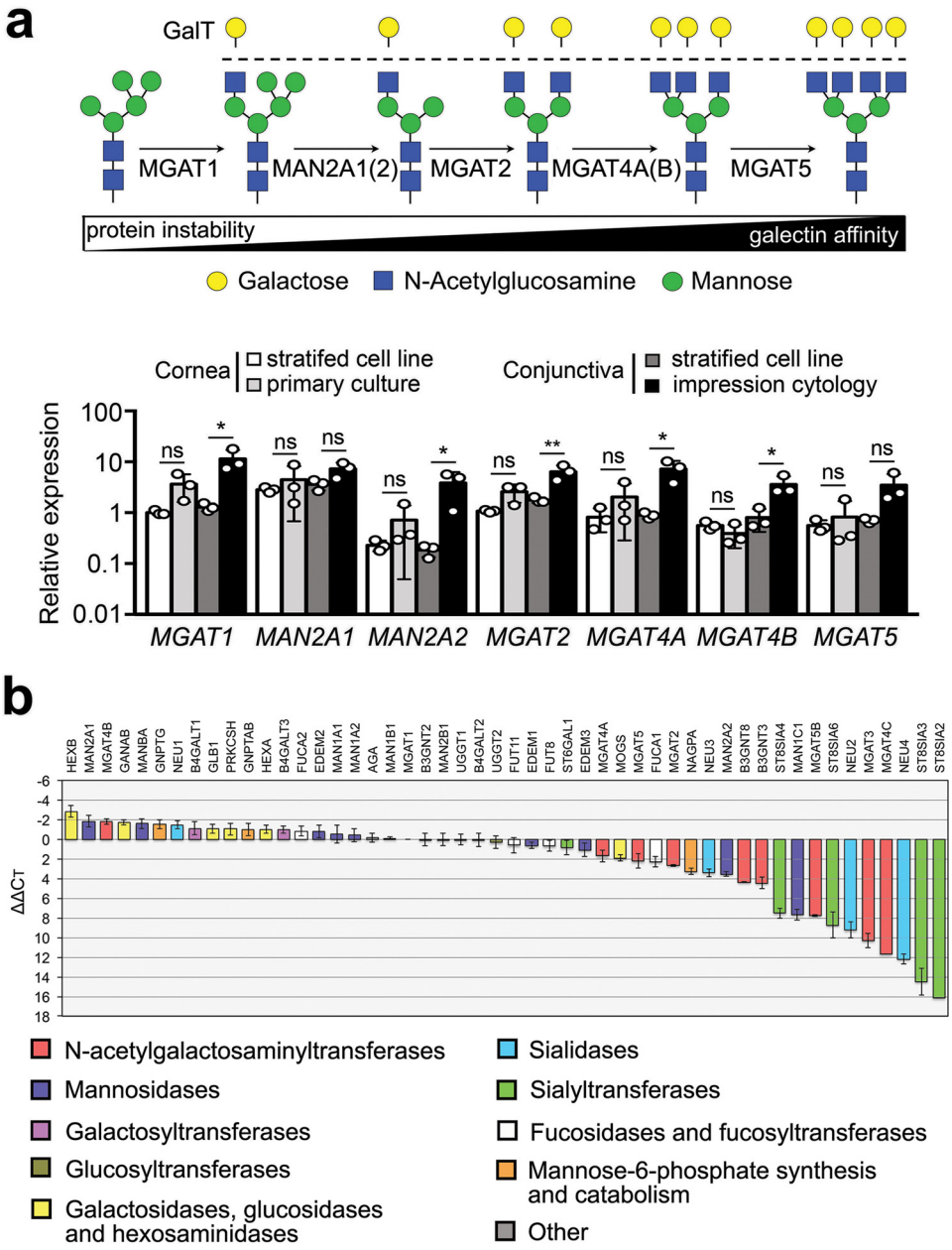

Figure 2. The GlcNAc-branching pathway in ocular surface epithelia. *a*, branches in complex-type *N*-glycans are processed through a series of enzymes, including MGAT1, MAN2A1, MAN2A2, MGAT2, MGAT4A, MGAT4B, and MGAT5 in the medial Golgi compartment. Gene expression of all of these enzymes was confirmed by qPCR in stratified human corneal and conjunctival cell lines, primary corneal epithelial cells, and native tissue (impression cytology) from human conjunctiva. *b*, the expression of *N*-glycan-processing genes in stratified cultures of human corneal epithelial cells was assessed by qPCR using a human glycosylation PCR array. The data show expression of B4GALT1 and B3GNT8, enzymes involved in the synthesis of poly-*N*-acetyllactosamine. In these experiments, negative or positive $\Delta\Delta C_T$ values indicate, respectively, whether expression of the gene of interest is higher or lower than the reference gene *MGAT1*. Results in *a* represent three independent experiments performed in duplicate or triplicate. Data are represented as the mean ± S.D. Significance was determined using one-way analysis of variance with Tukey's post hoc test. The array in *b* was repeated twice with independently isolated RNA pooled from three tissue culture plates. *, $p < 0.05$; **, $p < 0.01$; *ns*, nonsignificant. *GalT*, galactosyltransferase.

showed resemblance with those observed in native epithelia, although the expression of MGAT1, MAN2A2, MGAT2, MGAT4A, and MGAT4B in conjunctival epithelium was nearly an order of magnitude lower in the cell line than in native tissue. Additional analysis of *N*-glycan processing genes in human corneal epithelial cells by PCR array revealed the expression of B4GALT1 and B3GNT8 (Fig. 2*b*), enzymes involved in the synthesis of poly-*N*-acetyllactosamine (25, 26).

Characterization of mucin N-glycan structures by MALDI-TOF MS

To gain insight into the function of *N*-glycans in transmembrane mucins, we first examined their structure using mucin isolated from cultures of stratified human corneal epithelial cells. The purification protocol was based on a standard two-step procedure using size exclusion chromatography and isopycnic density centrifugation (27). PAS staining after chromatographic separation revealed the presence of carbohydrate-rich

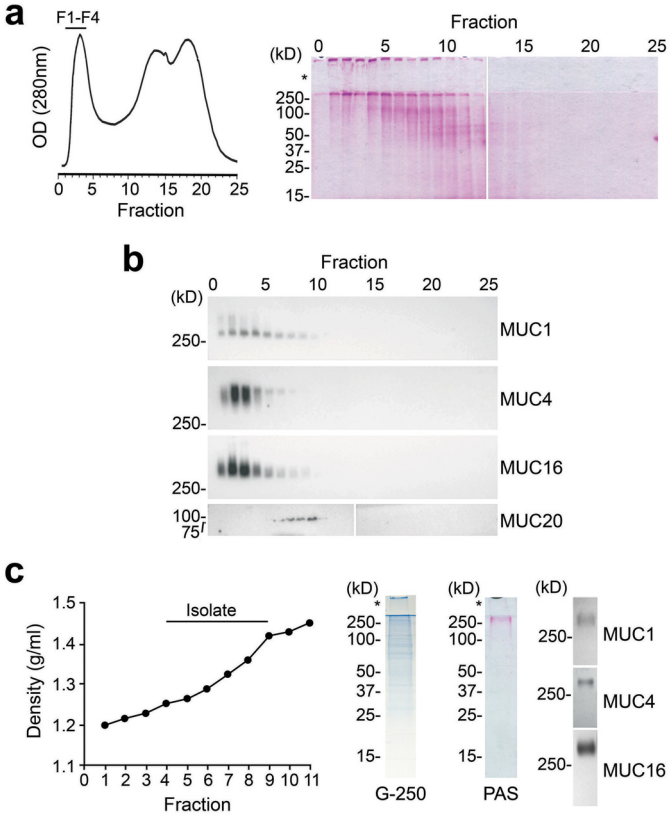

Figure 3. Purification of high-molecular-weight transmembrane mucins from stratified human corneal epithelial cells. An established two-step isolation procedure using size-exclusion chromatography and isopycnic density centrifugation was employed to purify transmembrane mucins. *a*, ~10 mg of cell extract was applied to a Sepharose CL-4B column (1 × 30 cm) and eluted with PBS, pH 7.5. Fractions were evaluated for glycoprotein content using PAS staining. The *asterisk* indicates the stacking gel. *b*, by Western blotting, the high-molecular-weight fractions F1-F4 contained MUC1, MUC4, and MUC16 but not the smaller MUC20 transmembrane mucin. *c*, these fractions were pooled and subjected to isopycnic density centrifugation. Fractions at a buoyant density range of 1.26–1.43 g/ml tested positive for MUC1, MUC4, and MUC16 and were combined for *N*-glycan sequencing analyses. Coomassie G-250 staining revealed the presence of some low-molecular-weight bands in the mucin isolate; however, these bands were not glycosylated, as shown by PAS staining.

bands in high-molecular-weight fractions (Fig. 3*a*). Western blotting analysis after agarose gel electrophoresis identified the mucins in these fractions to be MUC1, MUC4, and MUC16 (Fig. 3*b*). MUC1, -4, and -16 have been demonstrated at both the mRNA and protein levels in stratified corneal epithelium where they localize to the apical glycocalyx of superficial cells and participate in barrier function (28). MUC20, a small transmembrane mucin highly expressed at the ocular surface, eluted outside the high-molecular-weight region. MUC20 has been shown to localize primarily to cell membranes within intermediate cell layers and not the apical surface glycocalyx (29), and therefore, it was not included for analysis in the present study. The high-molecular-weight fractions (F1-F4) were pooled and further fractionated in an isopycnic cesium chloride gradient. Fractions with a buoyant density between 1.26 and 1.43 g/ml tested positive for MUC1, MUC4, and MUC16 (Fig. 3*c*) and were subjected to *N*-glycan analysis. As shown by Coomassie G-250 staining, some low-molecular-weight bands were present in the mucin isolates. However, we confirmed using PAS staining that these bands were not glycosylated and would not interfere with the glycan analysis, consistent with previous data (30).

Table 1
Carbohydrate compositions and relative intensities of the major peaks in the MALDI-TOF MS spectrum of transmembrane mucin *N*-glycans from human corneal epithelial cells

m/z[a]			
Observed	Theoretical	Composition	Relative intensity
			%
1580.3	1579.9	$Hex_5HexNAc_2$	55.3
1784.5	1784.0	$Hex_6HexNAc_2$	60.8
1988.6	1988.1	$Hex_7HexNAc_2$	75.3
2041.7	2040.2	$Hex_4HexNAc_4Fuc_1$	16.4
2071.7	2070.2	$Hex_5HexNAc_4$	26.7
2157.7	2156.2	$Hex_4HexNAc_3Fuc_1NeuAc_1$	17.3
2193.8	2192.2	$Hex_8HexNAc_2$	85.2
2245.8	2244.3	$Hex_5HexNAc_4Fuc_1$	64.7
2397.9	2396.3	$Hex_9HexNAc_2$	30.3
2418.9	2418.4	$Hex_5HexNAc_4Fuc_2$	24.8
2432.9	2431.4	$Hex_5HexNAc_4NeuAc_1$	62.1
2607.1	2605.5	$Hex_5HexNAc_4Fuc_1NeuAc_1$	100.0
2695.1	2693.5	$Hex_6HexNAc_5Fuc_1$	16.5
2794.2	2792.6	$Hex_5HexNAc_4NeuAc_2$	39.3
2968.3	2966.7 or 2968.7	$Hex_7HexNAc_6$ or $Hex_5HexNAc_4Fuc_1NeuAc_2$	53.3
3056.4	5054.7	$Hex_6HexNAc_5Fuc_1NeuAc_1$	22.2
3418.7	3415.9 or 3417.9	$Hex_6HexNAc_5Fuc_1NeuAc_2$ or $Hex_8HexNAc_7$	18.9
3506.8	3504.0	$Hex_7HexNAc_6Fuc_1NeuAc_1$	15.7
3868.1	3865.2	$Hex_7HexNAc_6Fuc_1NeuAc_2$	21.8
4229.4	4226.4	$Hex_7HexNAc_6Fuc_1NeuAc_3$	18.8

[a] All peaks were observed as $(M+Na)^+$ ions.

We performed the structural analysis of the *N*-glycans in human corneal mucins using mass spectrometry. The *N*-linked oligosaccharides in the mucin-enriched fraction were enzymatically released and permethylated before MALDI-TOF MS analysis. Data presented in Table 1 indicate that corneal mucins are characterized by the presence of complex-type *N*-glycans carrying *N*-acetyllactosamine residues ($Hex_{4-7}HexNAc_{3-6}$). The profile of the MS spectrum in the middle and high m/z regions consisted primarily of molecular ions that were consistent with bi-, tri-, and tetra-antennary complex glycans (Fig. 4), including structures carrying different numbers of putative *N*-acetyllactosamine repeats. The majority of the complex *N*-glycans was capped with sialic acid (*N*-acetylneuraminic acid) residues on their antennae ($n = 1–4$) and was also monofucosylated, suggesting core fucosylation (as Fuc-HexNAc at the reducing terminal). In addition, the results in the low mass region (m/z = 1580.3, 1784.5, 1988.6, 2193.8, and 2397.9) also provided indication that corneal mucins have compositions consistent with high mannose structures ($Hex_{5-9}HexNAc_2$). The hybrid-type *N*-glycans or bisecting GlcNAc structures represented a minor portion of the total *N*-glycan profile. Collectively, these results indicate that, consistent with the expression of *N*-acetylglucosaminyltransferase genes, complex-type *N*-glycan branching is a modification found on human corneal transmembrane mucins.

Abrogation of N-glycosylation impairs MUC16 stability and glycocalyx barrier function

With 250 potential *N*-glycosylation sites, MUC16 has the highest number of *N*-glycans per mucin molecule in corneal epithelium. To elucidate the role of *N*-glycans on MUC16, we treated stratified human corneal epithelial cell cultures with

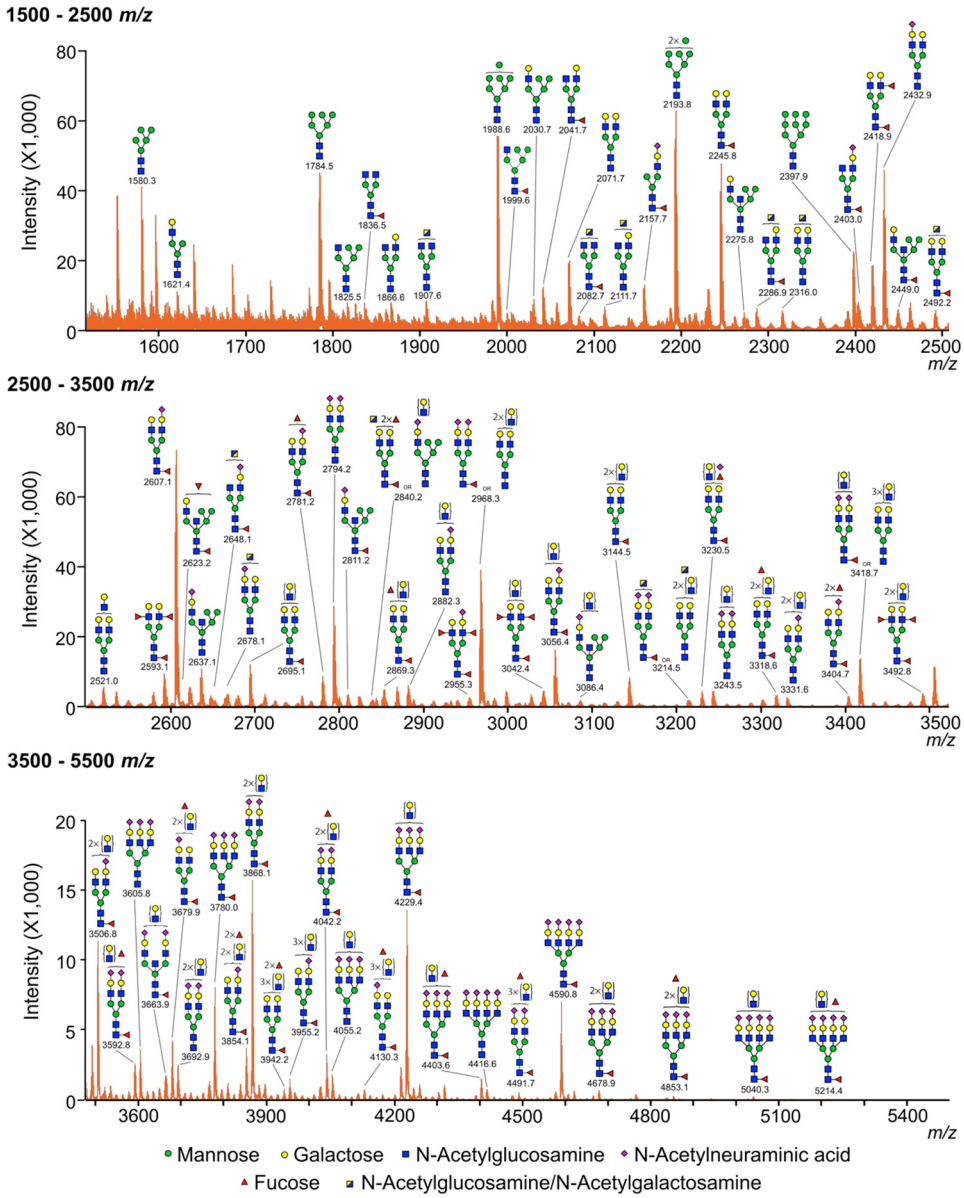

Figure 4. MALDI-TOF profile of *N*-glycans from transmembrane mucins isolated from human corneal epithelial cells. The *N*-linked glycans were released enzymatically by PNGase F, permethylated, and profiled by MALDI-TOF mass spectrometry. Magnified portions at m/z = 1500–2500, 2500–3500, and 3500–5500 are shown. Putative structures are assigned based on compositional information and known biosynthetic pathways. Most of the *N*-glycans on corneal mucins have compositions consistent with bi-, tri-, and tetra-antennary complex glycans, carrying *N*-acetyllactosamine residues and high mannose structures. All molecular ions detected are present in the form of $[M + Na]^+$.

tunicamycin, a potent inhibitor of *N*-linked glycosylation acting in the endoplasmic reticulum. This resulted in partial loss of binding to ConA, a plant lectin that specifically binds to mannose-rich carbohydrate cores in *N*-glycans, and a concomitant decrease in total and cell-surface expression of MUC16 (Fig. 5*a*). In addition, we used the rose bengal penetrance assay to provide evidence that inhibition of *N*-glycosylation impairs glycocalyx barrier function (Fig. 5*b*), which could be attributed to the overall loss of MUC16 glycans, both N- and *O*-linked. These results are in agreement with data showing that knockdown of MUC16 expression impairs corneal epithelial barrier function (31).

Furthermore, we employed an additional approach to evaluate the role of the Golgi *N*-glycan-branching pathway in maintaining MUC16 stability and function. Here, small interfering RNA (siRNA) technology was used to transiently knock down the *N*-acetylglucosaminyltransferase *MGAT1* in stratified cultures of human corneal epithelial cells. Compared with the scramble control, transfection with *MGAT1* siRNA resulted in a 5-fold decrease in *MGAT1* mRNA expression and a 2-fold reduction in PHA-L (*Phaseolus vulgaris* leucoagglutinin), a marker of GlcNAc-branching (Fig. 5*c*). Similar to our observations with tunicamycin, abrogation of *MGAT1* impaired the protein stability and cell-surface expression of MUC16 and was associated with reduced glycocalyx barrier function (Fig. 5, *d* and *e*). These results correlated with the transcriptional up-regulation of the molecular chaperone BiP and the transcription factor CHOP (Fig. 5*f*), indicative of cells undergoing endoplasmic reticulum stress and the activation of pathways within the unfolded protein response that prepare cells for apoptosis in

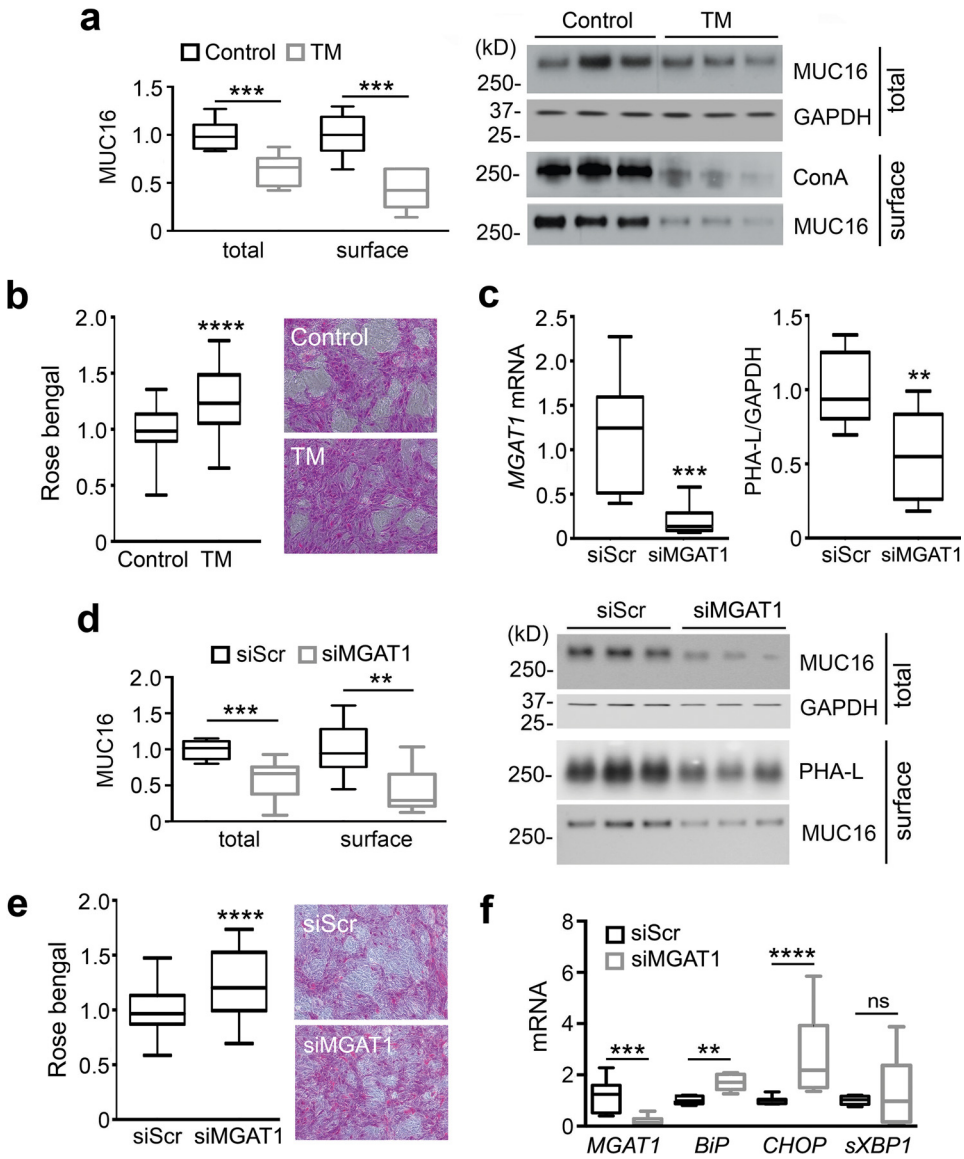

Figure 5. *N*-Glycosylation regulated MUC16 stability and the integrity of the corneal epithelial glycocalyx. *a*, tunicamycin (*TM*, 10 μg/ml) was added for the last 3 days of culture to inhibit synthesis of *N*-glycans in stratified human corneal epithelial cells. At the end of the incubation, cell-surface proteins were biotinylated at 4 °C, and an aliquot of ~20% of the total cell lysate was stored before pulldown. The biotinylated proteins were isolated using NeutrAvidin™. Under these conditions, tunicamycin decreased MUC16 levels both in the cell extracts and on the plasma membrane. Inhibition of *N*-glycosylation by tunicamycin in these experiments was evaluated using ConA. *b*, Rose bengal penetrance into epithelial cells significantly increased after treatment with tunicamycin. *c*, cultures of human corneal epithelial cells were transfected with either non-targeting scramble control (*siScr*) or *MGAT1*-targeting siRNA (*siMGAT1*). Reduction in the expression of *MGAT1* mRNA and *N*-glycan GlcNAc-branching was determined by qPCR and PHA-L (*P. vulgaris* leucoagglutinin) blot analysis, respectively. *d*, similar to tunicamycin, siRNA down-regulation of *MGAT1* reduced the total and cell-surface levels of MUC16 protein. *e*, suppression of *MGAT1* by siRNA was associated with an increase in Rose bengal penetrance into epithelial cells. *f*, the levels of *MGAT1*, *BiP*, *CHOP*, and *sXBP1* mRNA were determined by qPCR. Results in *a–f* represent three independent experiments performed in triplicate. The *box and whisker plots* show the 25 and 75 percentiles (*box*) and the median and the minimum and maximum data values (*whiskers*). Significance was determined using Student's *t* test. **, $p < 0.01$; ***, $p < 0.001$; ****, $p < 0.0001$; *ns*, nonsignificant.

the event of irrecoverable levels of stress (32). In these experiments, transfection with *MGAT1* siRNA did not significantly alter the expression of sXBP1, a component of the IRE1 (inositol-requiring transmembrane kinase/endonuclease 1) response involved in the activation of genes crucial for secretory function. Taken together, these data support the concept that *N*-glycans and the GlcNAc-branching pathway stimulate the integrity and protective role of MUC16 in corneal epithelium.

N-Glycans modulate the MUC16-galectin-3 interaction

To get insight into the mechanism by which mucin *N*-glycans promote glycocalyx barrier function, we investigated the contribution of *N*-glycosylation to the binding of MUC16 to galectin-3, an association that has been shown to have a protective effect on the epithelial cell surface (16, 17). For these experiments, a slot-blot galectin-3 binding assay was developed where recombinant human galectin-3 (rhGal-3) was directly immobilized onto membranes and probed with human corneal cell lysates treated with PNGase F, an enzyme causing *N*-glycan cleavage on glycoproteins. As shown in Fig. 6*a*, immobilized rhGal-3 was able to bind control MUC16 in a dose-dependent manner. In contrast, incubation of cell lysates with PNGase F significantly reduced the binding activity of MUC16 toward immobilized rhGal-3.

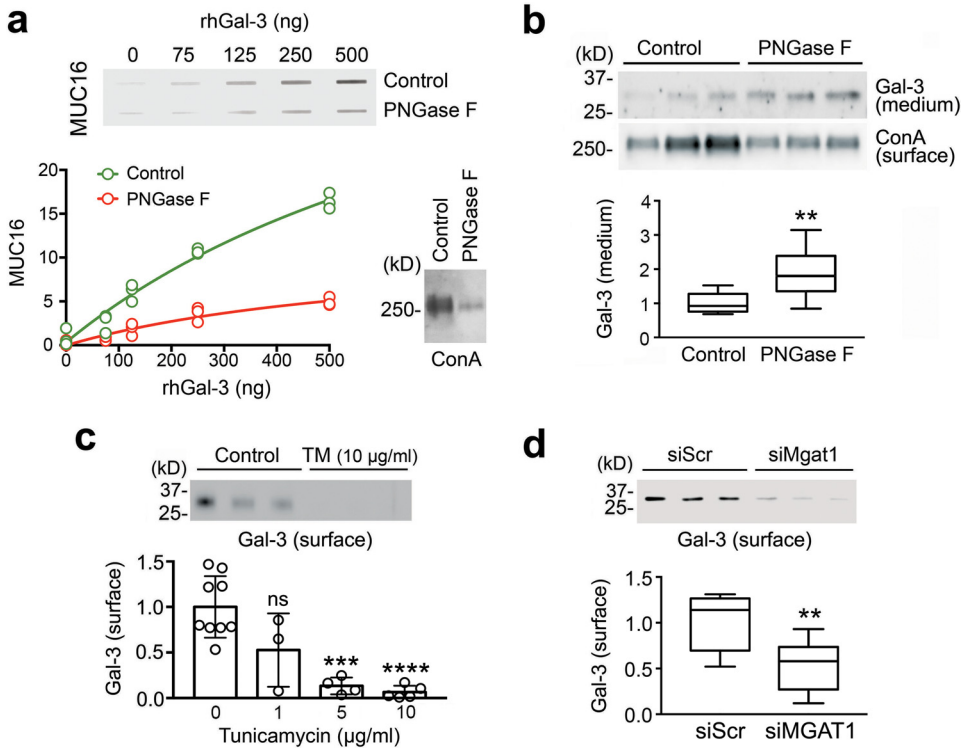

Figure 6. Galectin-3 interaction with MUC16 and its retention on the cell surface were *N*-glycan-dependent. *a*, 2-fold serial dilutions of rhGal-3 were applied individually to a nitrocellulose membrane in a slot-blot apparatus. Membranes were subsequently incubated with denatured cell lysates treated with or without PNGase F for 3 h at 37 °C. The enzymatic release of *N*-glycans significantly reduced the binding activity of MUC16 toward immobilized rhGal-3. Removal of *N*-glycans after PNGase F treatment was evaluated using ConA. *b*, treatment of stratified human corneal epithelial cells with PNGase F for 24 h significantly increased the amount of galectin-3 present in the cell culture medium. Relative amounts of *N*-glycans in biotinylated cell-surface proteins were evaluated using ConA. *c*, stratified human corneal epithelial cells were cultured in medium containing 1–10 μg/ml tunicamycin (*TM*) for the last 3 days of culture. Cells were then surface-labeled with biotin at 4 °C and pulled down using NeutrAvidin™. Galectin-3 was detected by Western blotting. *d*, cultures of human corneal epithelial cells were transfected with either non-targeting scramble control (*siScr*) or *MGAT1*-targeting siRNA (*siMGAT1*). As observed by cell-surface biotinylation and Western blotting, the knockdown of *MGAT1* decreased the abundance of cell-surface galectin-3. Results in *a* and *c* represent at least three independent experiments. Results in *b* and *d* represent three independent experiments performed in triplicate. Data in *c* are represented as the mean ± S.D. The *box and whisker plot* show the 25 and 75 percentiles (*box*) and the median and the minimum and maximum data values (*whiskers*). Significance was determined using Student's *t* test (*b* and *d*) and one-way analysis of variance with Tukey's post hoc test (*c*). **, $p < 0.01$; ***, $p < 0.001$; ****, $p < 0.0001$; *ns*, nonsignificant.

The enzymatic release of *N*-glycans by PNGase F was evidenced using ConA.

Furthermore, *N*-glycosylation inhibition experiments were performed in cell culture to address whether *N*-linked glycosylation is required to cause retention of galectin-3 on the epithelial cell surface. Treatment of stratified human corneal epithelial cells with PNGase F resulted in a significant reduction in cell-surface ConA-binding and a 2-fold increase in the amount of galectin-3 present in the cell culture medium (Fig. 6*b*). Additionally, we showed that the amount of galectin-3 present on the epithelial cell surface decreased in a dose-dependent manner after incubation of the cell cultures with tunicamycin (Fig. 6*c*). Finally, we investigated the role of the Golgi *N*-glycan branching pathway in this process. As shown in Fig. 6*d*, transient knockdown of *MGAT1* significantly reduced the amount of cell-surface galectin-3 compared with scramble control. Overall, these results demonstrate that mucin *N*-glycans and the GlcNAc-branching pathway are critical for maintaining the integrity of the corneal epithelial glycocalyx.

Discussion

Proper maintenance of mucosal homeostasis requires the establishment of diverse regulatory mechanisms that cooperatively protect against pathogenic and environmental challenges. These include secretion of a broad range of antimicrobial peptides aimed to shape the mucosal microenvironment and the modulation of the immune response when the integrity of the epithelium is compromised. The epithelium further contributes to provide a robust anatomical barrier by forming intercellular tight junctions and producing a dense glycocalyx on the apical surface composed of transmembrane mucins. Although the contribution of mucin *O*-glycans to the protection of mucosal surfaces has been extensively investigated, relatively little is known about the structure and function of mucin *N*-glycans in healthy epithelia. Here, we have characterized *N*-glycans associated to transmembrane mucins produced by differentiated human epithelial cells and have found a role for *N*-glycans and the Golgi *N*-glycan-branching pathway in maintaining MUC16 stability and the barrier function of the corneal glycocalyx.

Initial attempts using gel filtration chromatography to quantify the carbohydrate content of MUC16 isolated from OVCAR-3 ovarian cancer cells suggested that very few *N*-glycans were present on the mucin (12). These results have been subsequently challenged with more sensitive methods of detection, indicating that the content of *N*-glycans on MUC16 is

more abundant than initially thought. MALDI-TOF sequencing has established that MUC16 derived from OVCAR-3 cells is rich in *N*-glycans and has compositions consistent with complex-type glycans containing bisecting GlcNAc and high mannose-type structures (30). The most abundant complex-type *N*-glycans consisted of mono-fucosylated bisected bi-antennary structures, although tri- and tetra-antennary structures were also observed when analyzing high-molecular-mass components. The level of sialylation was relatively low, with no components carrying more than a single sialic acid, and there was evidence for fucose in the antennae other than the core. The presence of bisected bi-antennary structures in MUC16 has been further confirmed using serum from patients with ovarian cancer (33). Interestingly, our data indicate that transmembrane mucin *N*-glycans in differentiated human corneal epithelial cells contain primarily complex-type structures with *N*-acetyllactosamine. In contrast to OVCAR-3 cells, we have observed that bisecting GlcNAc represents a minor portion of the total glycan profile in corneal mucins, which are also characterized by the presence of more than one terminal sialic acid in the antennae. These structural differences and the proportion of each glycan may reflect specific requirements of individual epithelia, leading to precise cellular responses (14). Because of the lack of experimental data, little is known about the contribution of transmembrane mucin *N*-glycans to the requirements of individual epithelia. It is tempting to speculate that a lack of glycan chains containing bisecting GlcNAc in corneal epithelium is necessary for the maintenance of barrier integrity, as the introduction of bisecting GlcNAc into glycoproteins has been shown to negatively affect their interaction with galectins (34); yet this hypothesis remains untested.

Our results from tunicamycin-treated cells show that abrogation of *N*-glycosylation in the endoplasmic reticulum decreases total and cell-surface levels of MUC16 with a concomitant impairment of epithelial barrier function. These data are consistent with recent findings showing that defective *N*-glycosylation affects the stability of a recombinant 114-amino acid fragment within the C-terminal domain of MUC16 (35) and suggest that *N*-glycans are crucial to the function of native MUC16. To investigate the effects of the *N*-glycan branching pathway in MUC16 stability, we established a protocol to impair the expression of MGAT1, a resident Golgi glycosyltransferase that initiates complex *N*-linked oligosaccharide biosynthesis. The results indicated that, similar to *N*-glycan abrogation in the endoplasmic reticulum, knockdown of *MGAT1* in the Golgi was sufficient to reduce the stability of MUC16 and impair the barrier function of the epithelial glycocalyx. The ability of tunicamycin to impair MUC16 stability was expected based on its ability to induce protein misfolding in the endoplasmic reticulum, which could affect MUC16 itself or other proteins involved in MUC16 biosynthesis, leading to protein retrotranslocation into the cytosol and degradation via the ubiquitin-proteasome system (13). Indeed, the C-terminal region of MUC16 has been shown to be susceptible to ubiquitylation and proteasomal degradation (35). Even more intriguing was the observation that *MGAT1* down-regulation affects MUC16 protein integrity, as MGAT1 is a medial-Golgi enzyme and does not influence nascent protein folding. Previous observations in hepatocarcinoma cells have shown that suppression of *MGAT5*, a branching *N*-acetylglucosaminyltransferase acting on carbon 6 of α1,6-linked mannose, affects the function of *N*-glycan-synthesizing enzymes and chaperones and causes the unfolded protein response (36). In our experiments, knockdown of *MGAT1* led to transcriptional activation of *BiP* and *CHOP*, suggesting a model by which MGAT1 indirectly affects MUC16 stability by promoting endoplasmic reticulum stress and the activation of proteins involved in the recovery process.

The mechanism by which transmembrane mucin *N*-glycans stimulated glycocalyx barrier function could potentially involve interaction with galectin-3 on the epithelial surface. Several groups including ours have reported that *O*-glycans on transmembrane mucins allow interaction with galectins, such as MUC16 with galectin-1 and -3 (16, 37), which in the cornea promote the formation of protective lattices. Despite these findings, studies both *in vitro* and *in vivo* support the concept that interaction with galectins may also depend on the presence of *N*-glycans on transmembrane mucins. Although limited by the conformational constraints of artificial formats, experiments with synthetic glycan microarrays have shown that galectin-3 displays maximum binding affinity toward *N*-glycans compared with *O*-glycans (38). These studies have been supported by the use of CHO glycosylation mutants with various repertoires of cell surface glycans indicating that complex *N*-glycans are the preferred ligands for galectins (39). It is possible to speculate that the presence of putative *N*-glycosylation sites within the MUC16 tandem repeat would contribute to promote interaction with galectins, as the affinity of lectins toward glycoproteins is associated with the density and number of glycan epitopes and not just the structure of a single epitope (40). In this study we show that *N*-acetyllactosamine is a common structure found in corneal mucin *N*-glycans and that PNGase F removal of *N*-glycans reduces the affinity of MUC16 toward galectin-3, findings that implicate *N*-glycosylation in modulating the mucin-galectin lattice. Furthermore, we show that *N*-glycans in general and MGAT1 in particular are important for the normal expression of galectin-3 on the cell surface, suggesting that complex *N*-glycans on MUC16 contribute to sustain glycocalyx barrier function in the cornea via retention of galectin-3. Outstanding questions remain regarding the relative contributions of *N*- and *O*-glycans in modulating the overall affinity of transmembrane mucins toward galectins, including the enzymes controlling their biosynthesis and whether they play non-redundant roles during corneal homeostasis. These investigations will help to define the importance of these pathways and the therapeutic potential of their stimulation in reversing ocular surface epithelial dysfunction.

Experimental procedures

Cell culture and reagents

Telomerase-immortalized human corneal and conjunctival epithelial cells were grown in keratinocyte serum-free medium (KSFM; Thermo Fisher Scientific, Rockford, IL) supplemented with bovine pituitary extract, 0.2 ng/ml epithelium growth factor (EGF), and 0.4 mM $CaCl_2$ at 37 °C in 5% CO_2. Once confluent, cells were switched to Dulbecco's modified Eagle's medium

(DMEM)/F-12 supplemented with 10% newborn calf serum and 10 ng/ml EGF for 7 days to promote cell stratification and establishment of barrier function (41). These cell lines were derived from normal tissue and expressed the same mucin gene and keratin repertoire as native epithelia (42). Human corneal epithelial explant cultures were generated from residual corneoscleral rims obtained as discarded samples from an unrelated study. Human conjunctival impression cytology samples were obtained as archived material from a previously published study (43). rhGal-3 was expressed as previously reported by the addition of 0.3 mM isopropyl β-D-1-thiogalactopyranoside (IPTG) to Rosetta™ *Escherichia coli* clones carrying a galectin-3 expression vector (17). The rhGal-3 was purified from lysates by affinity chromatography using lactosyl-Sepharose. To eliminate contaminating bacterial endotoxins, rhGal-3 was further purified by polymyxin B affinity chromatography. The absence of lipopolysaccharide was confirmed using the ToxinSensor™ Chromogenic LAL Endotoxin Assay kit (GenScript, Piscataway, NJ). Protein solutions were concentrated by filtration (VIVASPIN, Littleton, MA) dialyzed against phosphate-buffered saline (PBS) buffer containing 10% glycerol and stored at −20 °C. *N*- and *O*-glycosylation sites on the full-length sequences of human MUC1, MUC4, and MUC16 were analyzed using the artificial neural networks NetNGlyc 1.0 and NetOGlyc 4.0 (Center for Biological Sequence Analysis, Technical University of Denmark, Lyngby, Denmark), respectively.

Mucin purification

Transmembrane mucins were purified from stratified corneal epithelial cell cultures as previously described (44). Briefly, protein from cell cultures was extracted using radioimmune precipitation assay buffer (150 mM NaCl, 25 mM Tris-HCl, pH 7.6, 1% Nonidet P-40, 1% sodium deoxycholate, 0.1% SDS) plus Complete™ EDTA-free Protease Inhibitor Mixture (Roche Diagnostics). After homogenization with a pellet pestle, the protein extract was centrifuged at 17,115 × *g* for 45 min at 4 °C, and the protein concentration of the supernatant was determined using the Pierce BCA Protein Assay Kit (Thermo Fisher Scientific). Proteins were size-fractionated by gel chromatography on a Sepharose CL-4B column. Fractions containing the high-molecular-weight mucins were pooled and digested with RNase A and DNase I for 3 h at room temperature and further purified by isopycnic density gradient centrifugation in cesium chloride at 164,000 × *g* for 72 h at 4 °C. Mucins resolved in the middle of the density gradient were pooled, dialyzed, and stored at −80 °C before *N*-glycan structural analysis. The protein concentration in mucin isolate was measured using the Micro BCA Protein Assay kit (Thermo Fisher Scientific). PAS stain (GelCode Glycoprotein Stain, Thermo Fisher Scientific) and Coomassie G-250 (GelCode Blue Safe Protein Stain, Thermo Fisher Scientific) were used to monitor carbohydrate and protein content after SDS-PAGE (10% resolving gel), respectively, whereas Western blotting was used to monitor transmembrane mucin content following agarose gel electrophoresis.

Cell-surface protein biotinylation

Before biotinylation, the medium was discarded, and the cultures were serum-starved for 2 h. Cells were then surface-labeled with the Pierce® Cell Surface Protein Isolation kit (Thermo Fisher Scientific) following the manufacturer's instructions. Briefly, cells were incubated with 0.25 mg/ml cell-impermeable sulfo-NHS-SS-Biotin at 4 °C for 30 min. After quenching the reaction and washing with Tris-buffered saline (TBS), cells were lysed in the presence of Halt Protease Inhibitor Mixture (Thermo Fisher Scientific). Lysates were incubated with 100 μl of NeutrAvidin™ for 1 h at room temperature. Biotinylated proteins were eluted with dithiothreitol.

Inhibition of N-glycosylation and enzymatic deglycosylation

To inhibit *N*-glycosylation, cells were cultured in medium containing 1–10 μg/ml tunicamycin (Sigma) for the last 3 days of culture. For enzymatic deglycosylation of cell lysates, proteins (0.5 mg) were denatured by boiling for 5 min at 95 °C in buffer containing 52 mM β-mercaptoethanol and 0.1% SDS. The denatured samples were treated with 10 μl of PNGase F (5 units/μl) from *Elizabethkingia meningoseptica* (Sigma) for 3 h at 37 °C in the presence of 0.75% Triton X-100. Enzymatically-cleaved glycans were removed by filtration in a NanoSep 10K column (VIVASPIN). Proteins on the membrane were recovered using PBST (PBS + 0.1% Triton X- 100) and stored at −80 °C before galectin-3-binding assay. For PNGase F treatment of live cells, cultures were washed 3 times with PBS and incubated with 10 units/ml PNGase F in DMEM/F-12 at 37 °C for the last day of culture as described (45).

For structural analyses, mucin isolates (40 μg) were lyophilized, reduced in 500 μl of a 2 mg/ml dithiothreitol solution at 50 °C for 90 min, and then alkylated with 500 μl of a 12 mg/ml iodoacetamide (Sigma) solution for 90 min at room temperature in the dark. The sample was dialyzed against 50 mM ammonium bicarbonate for 24 h at 4 °C, lyophilized, and incubated with 1 ml of 50 μg/ml TPCK (tosylphenylalanyl chloromethyl ketone)-treated trypsin (Sigma) at 37 °C overnight. The digested peptides were then purified using a Sep-Pak C18 (200 mg) cartridge (Waters Corp., Milford, MA), lyophilized, and incubated with 2 μl (500units/μl) of PNGase F from *Flavobacterium meningosepticum* (P0704, New England Biolabs, Ipswich, MA) in 200 μl of 50 mM ammonium bicarbonate at 37 °C for 4 h. The mixture was further incubated with 3 μl of PNGase F at 37 °C overnight. The released *N*-glycans were purified over a Sep-Pak C18 (200 mg) cartridge. The flow-through and wash fraction containing the released *N*-glycans were collected, pooled, and lyophilized.

Permethylation of N-glycans

To enhance the sensitivity of *N*-glycan analysis by mass spectrometry, permethylation of *N*-glycans was carried out using the NaOH:DMSO slurry method. Here, lyophilized *N*-glycans were incubated with 1 ml of a NaOH:DMSO slurry solution and 500 μl of methyl iodide (Sigma) for 20–30 min under vigorous shaking at room temperature. One ml of chloroform and 3 ml of Milli-Q water were then added, and the mixture was briefly vortexed to wash the chloroform fraction. The wash step was repeated 3 times. The chloroform fraction was dried, dissolved in 200 ml of 50% methanol, and loaded into a Sep-Pak C18 (200 mg) cartridge. The eluted fraction was lyophilized and dissolved in 10 μl of 75% methanol from which 1 μl was mixed

with 1 μl 2,5-dihydroxybenzoic acid (Sigma) (5 mg/ml in 50% acetonitrile with 0.1% trifluoroacetic acid) and spotted on a MALDI polished steel target plate (Bruker Daltonics, Bremen, Germany).

MALDI-TOF mass spectrometry

The profiling of permethylated *N*-glycans was performed at the Glycomics Core at Beth Israel Deaconess Medical Center, Boston. Mass spectrometry data were acquired on an UltraFlex II MALDI-TOF Mass Spectrometer (Bruker Daltonics). Reflective positive mode was used, and data were recorded between 500 m/z and 6000 m/z. The mass spectrometry *N*-glycan profile was acquired by the aggregation of at least 20,000 laser shots. MS spectra were processed using mMass (46). Mass peaks were manually annotated and assigned to a particular *N*-glycan composition when a match was found.

MGAT1 siRNA

Depletion of *MGAT1* was achieved using the Silencer® Select Pre-designed siRNA (s8728; Thermo Fisher Scientific) targeting a sequence of human *MGAT1* mRNA (5′-UGAGGACCAAUGACCGGAAtt-3′). A nonspecific scrambled siRNA (4390843; Life Technologies) served as the negative control. For knockdown, cells in 12-well plates were transfected twice, at confluence and 3 days post-confluence, by 6-h incubation with 10 μl of siRNA in Lipofectamine 2000 (Life Technologies; 2 μl) dissolved in 400 μl of Opti-MEM plus GlutaMax reduced-serum medium (Thermo Fisher Scientific). Cells were allowed to recover in supplemented DMEM/F-12 medium for 72 h after each transfection.

Western blotting and lectin blotting

Cell extracts were obtained by lysis in radioimmune precipitation assay buffer supplemented with Complete™ EDTA-free Protease Inhibitor Mixture (Roche Diagnostics). After homogenization with a pellet pestle, the cell extracts were centrifuged at 17,115 × *g* for 30 min at 4 °C, and the protein concentration of the supernatant was determined using the Pierce BCA™ Protein Assay Kit (Thermo Fisher Scientific). For analyses of cell culture medium, cells were washed with PBS followed by incubation with serum-free DMEM/F12 for 24 h at 37 °C. Medium was collected and centrifuged at 6,000 × *g* for 4 min to remove cellular debris.

For analysis of MUC1, MUC4, and MUC16, proteins were separated by 1% agarose gel electrophoresis and blotted onto nitrocellulose membranes using a vacuum as described (16). For analysis of MUC20, galectin-3, and GAPDH, proteins were separated by SDS-PAGE (10% resolving gel) and electroblotted onto nitrocellulose membranes. Nonspecific binding to the nitrocellulose was blocked at room temperature by 1 h of incubation with 5% nonfat milk in PBS for detection of MUC1 and MUC4 or 0.1% Tween 20 in Tris-buffered saline (TTBS) for detection of MUC16, MUC20, galectin-3, and GAPDH. Membranes were then incubated with primary antibodies to MUC1 (214D4, 1:3000; Upstate, Lake Placid, NY), MUC4 (8G7, 1:1000; Santa Cruz Biotechnology, Dallas, TX), MUC16 (M11, 1:3000; Neomarkers, Fremont, CA), MUC20 (RB13033, 1:3000; Abgent, San Diego, CA), and galectin-3 (H160; 1:3000; Santa Cruz Biotechnology) in blocking buffer overnight at 4 °C. GAPDH staining (1:5000; FL-335; Santa Cruz Biotechnology, Dallas, TX) served as a sample loading control. After washing with TTBS, membranes were incubated with the appropriate secondary antibodies coupled to horseradish peroxidase (1:5000; Santa Cruz Biotechnology) for 1 h at room temperature. Peroxidase activity was visualized using the West Pico Chemiluminescent Substrate (Thermo Fisher Scientific) according to the manufacturer's instructions. Densitometry was performed using ImageJ software (National Institutes of Health, Bethesda, MD).

For lectin blotting, proteins were separated by 1% agarose gel electrophoresis, blotted onto nitrocellulose membranes, and blocked with 1% polyvinylpyrrolidine in TTBS overnight at 4 °C. Membranes were then incubated with biotin-labeled concanavalin A (0.5 μg/ml; Vector Laboratories, Burlingame, CA) or *P. vulgaris* leucoagglutinin (5 μg/ml; Vector Laboratories) for 1.5 h at room temperature. Membranes were developed with the Vectastain ABC kit (Vector Laboratories), and glycoproteins were visualized using chemiluminescence.

Slot blot galectin-3 binding assay

Two-fold serial dilutions of rhGal-3 were applied individually to a nitrocellulose membrane in a slot-blot apparatus (Bio-Rad). Individual wells were overlaid for 30 min with 10 μg of cell lysate in 200 μl of TBS. The membranes were then blocked with 1% polyvinylpyrrolidine in TTBS for 45 min, washed thoroughly, and probed with the MUC16 primary antibody for 45 min. After washes with TBS, membranes were incubated with goat anti-mouse IgG (1:5000; Santa Cruz Biotechnology, Santa Cruz, CA) for another 45 min. Antibody binding was detected using chemiluminescence.

qPCR

Total RNA was isolated from cell cultures and impression cytology samples using the extraction reagent TRIzol (Thermo Fisher Scientific) following the manufacturer's instructions. Residual genomic DNA was eliminated by DNase I digestion of the RNA preparation. One μg of total RNA was used for cDNA synthesis (iScript™ cDNA Synthesis; Bio-Rad). Primer sequences used to amplify the *MGAT1*, *MAN2A1*, *MAN2A2*, *MGAT2*, *MGAT4A*, *MGAT4B*, *MGAT5*, binding immunoglobulin protein (*BiP*), CCAAT-enhancer-binding protein homologous protein (*CHOP*), and spliced X-box binding protein 1 (*sXBP1*) mRNA are listed in supplemental Table 1. Gene expression was measured using the KAPA SYBR® FAST qPCR kit (Kapa Biosystems, Wilmington, MA) in a Mastercycler ep realplex thermal cycler (Eppendorf, Hauppauge, NY). The following parameters were used: 2 min at 95 °C followed by 40 cycles of 5 s at 95 °C and 30 s at 60 °C. Expression values were corrected for the housekeeping gene *GAPDH* (PrimePCR GAPDH primers; Bio-Rad) and normalized using *MGAT1* as a reference gene. Fold changes were calculated using the comparative C_T method.

Human glycosylation PCR array

The expression of *N*-glycan-processing genes in stratified cultures of human corneal epithelial cells was assessed by qPCR

using a human glycosylation PCR array (RT^2 Profiler^{TM} PCR array, SABiosciences Corp., Frederick, MD) according to the manufacturer's instructions. Expression values were corrected for the housekeeping gene *GAPDH* and normalized using *MGAT1* as a reference gene. The $\Delta\Delta C_T$ method was used for relative quantitation of the number of transcripts.

Barrier function assay

Transcellular barrier function in cell culture was assayed with the rose bengal anionic dye (Acros Organics; Morris Plains, NJ) as described previously (41). For dye penetrance assay, cells in tissue culture plates were rinsed with PBS and incubated for 5 min with a 0.1% solution of Rose bengal. Afterward, the dye was aspirated, and the culture was further washed with PBS. The extent of dye penetrance in cell culture was assessed using an inverted microscope (Nikon Eclipse TS100). Pictures were taken at 10× with a SPOT Insight Fire Wire Camera (Diagnostic Instruments, Inc., Sterling Heights, MI) and analyzed using ImageJ software.

Statistical analyses

Statistical analyses were performed using Prism 7 (Graphpad Software, San Diego, CA) for Mac OSX.

Author contributions—T. T. and A. M. W. designed, performed, and interpreted the experiments. T. T. co-wrote the manuscript. P. M., N. M. M., and S. L. performed and interpreted the experiments and reviewed the manuscript. S. M. P. J. and J. M. assisted in experimental design and data interpretation and reviewed the manuscript. P. A. conceived the project, designed and interpreted the experiments, and co-wrote the manuscript.

Acknowledgments—We thank Ilene Gipson for providing the human corneal and conjunctival epithelial cell lines. We also thank Miguel González-Andrades for providing primary cultures of human corneal epithelial cells. We thank Sandra Spurr-Michaud and Ann Tisdale for technical assistance.

References

1. McGuckin, M. A., Lindén, S. K., Sutton, P., and Florin, T. H. (2011) Mucin dynamics and enteric pathogens. *Nat. Rev. Microbiol.* **9,** 265–278
2. Corfield, A. P. (2015) Mucins: a biologically relevant glycan barrier in mucosal protection. *Biochim. Biophys. Acta* **1850,** 236–252
3. Hilkens, J., Ligtenberg, M. J., Vos, H. L., and Litvinov, S. V. (1992) Cell membrane-associated mucins and their adhesion-modulating property. *Trends Biochem. Sci.* **17,** 359–363
4. Wesseling, J., van der Valk, S. W., Vos, H. L., Sonnenberg, A., and Hilkens, J. (1995) Episialin (MUC1) overexpression inhibits integrin-mediated cell adhesion to extracellular matrix components. *J. Cell Biol.* **129,** 255–265
5. Bafna, S., Kaur, S., and Batra, S. K. (2010) Membrane-bound mucins: the mechanistic basis for alterations in the growth and survival of cancer cells. *Oncogene* **29,** 2893–2904
6. Haridas, D., Ponnusamy, M. P., Chugh, S., Lakshmanan, I., Seshacharyulu, P., and Batra, S. K. (2014) MUC16: molecular analysis and its functional implications in benign and malignant conditions. *FASEB J.* **28,** 4183–4199
7. Chachadi, V. B., Bhat, G., and Cheng, P. W. (2015) Glycosyltransferases involved in the synthesis of MUC-associated metastasis-promoting selectin ligands. *Glycobiology* **25,** 963–975
8. Einerhand, A. W., Renes, I. B., Makkink, M. K., van der Sluis, M., Büller, H. A., and Dekker, J. (2002) Role of mucins in inflammatory bowel disease: important lessons from experimental models. *Eur. J. Gastroenterol. Hepatol.* **14,** 757–765
9. Gipson, I. K. (2013) Age-related changes and diseases of the ocular surface and cornea. *Invest. Ophthalmol. Vis. Sci.* **54,** ORSF48–53
10. Dogru, M., Matsumoto, Y., Okada, N., Igarashi, A., Fukagawa, K., Shimazaki, J., Tsubota, K., and Fujishima, H. (2008) Alterations of the ocular surface epithelial MUC16 and goblet cell MUC5AC in patients with atopic keratoconjunctivitis. *Allergy* **63,** 1324–1334
11. Hollingsworth, M. A., and Swanson, B. J. (2004) Mucins in cancer: protection and control of the cell surface. *Nat. Rev. Cancer* **4,** 45–60
12. Lloyd, K. O., Yin, B. W., and Kudryashov, V. (1997) Isolation and characterization of ovarian cancer antigen CA 125 using a new monoclonal antibody (VK-8): identification as a mucin-type molecule. *Int. J. Cancer* **71,** 842–850
13. Freeze, H. H., Esko, J. D., and Parodi, A. J. (2009) Glycans in glycoprotein quality control. In *Essentials of Glycobiology* (Varki, A., Cummings, R. D., Esko, J. D., Freeze, H. H., Stanley, P., Bertozzi, C. R., Hart, G. W., and Etzler, M. E., eds) 2nd Ed., pp. 513–521, Cold Spring Harbor Laboratory Press, Cold Spring Harbor, NY
14. Lau, K. S., Partridge, E. A., Grigorian, A., Silvescu, C. I., Reinhold, V. N., Demetriou, M., and Dennis, J. W. (2007) Complex *N*-glycan number and degree of branching cooperate to regulate cell proliferation and differentiation. *Cell* **129,** 123–134
15. Partridge, E. A., Le Roy, C., Di Guglielmo, G. M., Pawling, J., Cheung, P., Granovsky, M., Nabi, I. R., Wrana, J. L., and Dennis, J. W. (2004) Regulation of cytokine receptors by Golgi *N*-glycan processing and endocytosis. *Science* **306,** 120–124
16. Argüeso, P., Guzman-Aranguez, A., Mantelli, F., Cao, Z., Ricciuto, J., and Panjwani, N. (2009) Association of cell surface mucins with galectin-3 contributes to the ocular surface epithelial barrier. *J. Biol. Chem.* **284,** 23037–23045
17. Mauris, J., Mantelli, F., Woodward, A. M., Cao, Z., Bertozzi, C. R., Panjwani, N., Godula, K., and Argüeso, P. (2013) Modulation of ocular surface glycocalyx barrier function by a galectin-3 N-terminal deletion mutant and membrane-anchored synthetic glycopolymers. *PLoS ONE* **8,** e72304
18. Merlin, J., Stechly, L., de Beaucé, S., Monté, D., Leteurtre, E., van Seuningen, I., Huet, G., and Pigny, P. (2011) Galectin-3 regulates MUC1 and EGFR cellular distribution and EGFR downstream pathways in pancreatic cancer cells. *Oncogene* **30,** 2514–2525
19. Mori, Y., Akita, K., Yashiro, M., Sawada, T., Hirakawa, K., Murata, T., and Nakada, H. (2015) Binding of galectin-3, a β-galactoside-binding lectin, to MUC1 protein enhances phosphorylation of extracellular signal-regulated kinase 1/2 (ERK1/2) and Akt, promoting tumor cell malignancy. *J. Biol. Chem.* **290,** 26125–26140
20. Sindrewicz, P., Lian, L. Y., and Yu, L. G. (2016) Interaction of the oncofetal Thomsen-Friedenreich antigen with galectins in cancer progression and metastasis. *Front. Oncol.* **6,** 79
21. Gipson, I. K., and Argüeso, P. (2003) Role of mucins in the function of the corneal and conjunctival epithelia. *Int. Rev. Cytol.* **231,** 1–49
22. Dharmaraj, N., Chapela, P. J., Morgado, M., Hawkins, S. M., Lessey, B. A., Young, S. L., and Carson, D. D. (2014) Expression of the transmembrane mucins, MUC1, MUC4. and MUC16, in normal endometrium and in endometriosis. *Hum. Reprod.* **29,** 1730–1738
23. Hattrup, C. L., and Gendler, S. J. (2008) Structure and function of the cell surface (tethered) mucins. *Annu. Rev. Physiol.* **70,** 431–457
24. Yin, B. W., and Lloyd, K. O. (2001) Molecular cloning of the CA125 ovarian cancer antigen: identification as a new mucin, MUC16. *J. Biol. Chem.* **276,** 27371–27375
25. Ishida, H., Togayachi, A., Sakai, T., Iwai, T., Hiruma, T., Sato, T., Okubo, R., Inaba, N., Kudo, T., Gotoh, M., Shoda, J., Tanaka, N., and Narimatsu, H. (2005) A novel β1,3-*N*-acetylglucosaminyltransferase (β3Gn-T8), which synthesizes poly-*N*-acetyllactosamine, is dramatically upregulated in colon cancer. *FEBS Lett.* **579,** 71–78
26. Ujita, M., McAuliffe, J., Hindsgaul, O., Sasaki, K., Fukuda, M. N., and Fukuda, M. (1999) Poly-*N*-acetyllactosamine synthesis in branched *N*-glycans is controlled by complemental branch specificity of I-exten-

sion enzyme and β1,4-galactosyltransferase I. *J. Biol. Chem.* **274,** 16717–16726
27. Argüeso, P., and Gipson, I. K. (2006) Quantitative analysis of mucins in mucosal secretions using indirect enzyme-linked immunosorbent assay. *Methods Mol. Biol.* **347,** 277–288
28. Mantelli, F., and Argüeso, P. (2008) Functions of ocular surface mucins in health and disease. *Curr. Opin. Allergy Clin. Immunol.* **8,** 477–483
29. Woodward, A. M., and Argüeso, P. (2014) Expression analysis of the transmembrane mucin MUC20 in human corneal and conjunctival epithelia. *Invest. Ophthalmol. Vis. Sci.* **55,** 6132–6138
30. Kui Wong, N., Easton, R. L., Panico, M., Sutton-Smith, M., Morrison, J. C., Lattanzio, F. A., Morris, H. R., Clark, G. F., Dell, A., and Patankar, M. S. (2003) Characterization of the oligosaccharides associated with the human ovarian tumor marker CA125. *J. Biol. Chem.* **278,** 28619–28634
31. Blalock, T. D., Spurr-Michaud, S. J., Tisdale, A. S., Heimer, S. R., Gilmore, M. S., Ramesh, V., and Gipson, I. K. (2007) Functions of MUC16 in corneal epithelial cells. *Invest. Ophthalmol. Vis. Sci.* **48,** 4509–4518
32. Todd, D. J., Lee, A. H., and Glimcher, L. H. (2008) The endoplasmic reticulum stress response in immunity and autoimmunity. *Nat. Rev. Immunol.* **8,** 663–674
33. Saldova, R., Struwe, W. B., Wynne, K., Elia, G., Duffy, M. J., and Rudd, P. M. (2013) Exploring the glycosylation of serum CA125. *Int. J. Mol. Sci.* **14,** 15636–15654
34. Miwa, H. E., Song, Y., Alvarez, R., Cummings, R. D., and Stanley, P. (2012) The bisecting GlcNAc in cell growth control and tumor progression. *Glycoconj. J.* **29,** 609–618
35. Das, S., Majhi, P. D., Al-Mugotir, M. H., Rachagani, S., Sorgen, P., and Batra, S. K. (2015) Membrane proximal ectodomain cleavage of MUC16 occurs in the acidifying Golgi/post-Golgi compartments. *Sci. Rep.* **5,** 9759
36. Fang, H., Huang, W., Xu, Y. Y., Shen, Z. H., Wu, C. Q., Qiao, S. Y., Xu, Y., Yu, L., and Chen, H. L. (2006) Blocking of *N*-acetylglucosaminyltransferase V induces cellular endoplasmic reticulum stress in human hepatocarcinoma 7,721 cells. *Cell Res.* **16,** 82–92
37. Seelenmeyer, C., Wegehingel, S., Lechner, J., and Nickel, W. (2003) The cancer antigen CA125 represents a novel counter receptor for galectin-1. *J. Cell Sci.* **116,** 1305–1318
38. Stowell, S. R., Arthur, C. M., Mehta, P., Slanina, K. A., Blixt, O., Leffler, H., Smith, D. F., and Cummings, R. D. (2008) Galectin-1, -2, and -3 exhibit differential recognition of sialylated glycans and blood group antigens. *J. Biol. Chem.* **283,** 10109–10123
39. Patnaik, S. K., Potvin, B., Carlsson, S., Sturm, D., Leffler, H., and Stanley, P. (2006) Complex *N*-glycans are the major ligands for galectin-1, -3, and -8 on Chinese hamster ovary cells. *Glycobiology* **16,** 305–317
40. Dam, T. K., and Brewer, C. F. (2010) Lectins as pattern recognition molecules: the effects of epitope density in innate immunity. *Glycobiology* **20,** 270–279
41. Argüeso, P., and Gipson, I. K. (2012) Assessing mucin expression and function in human ocular surface epithelia *in vivo* and *in vitro*. *Methods Mol. Biol.* **842,** 313–325
42. Gipson, I. K., Spurr-Michaud, S., Argüeso, P., Tisdale, A., Ng, T. F., and Russo, C. L. (2003) Mucin gene expression in immortalized human corneal-limbal and conjunctival epithelial cell lines. *Invest. Ophthalmol. Vis. Sci.* **44,** 2496–2506
43. Uchino, Y., Mauris, J., Woodward, A. M., Dieckow, J., Amparo, F., Dana, R., Mantelli, F., and Argüeso, P. (2015) Alteration of galectin-3 in tears of patients with dry eye disease. *Am. J. Ophthalmol.* **159,** 1027–1035
44. Bravo-Osuna, I., Noiray, M., Briand, E., Woodward, A. M., Argüeso, P., Molina Martínez, I. T., Herrero-Vanrell, R., and Ponchel, G. (2012) Interfacial interaction between transmembrane ocular mucins and adhesive polymers and dendrimers analyzed by surface plasmon resonance. *Pharm. Res.* **29,** 2329–2340
45. Zhang, Z., Sun, J., Hao, L., Liu, C., Ma, H., and Jia, L. (2013) Modification of glycosylation mediates the invasive properties of murine hepatocarcinoma cell lines to lymph nodes. *PLoS ONE* **8,** e65218
46. Strohalm, M., Kavan, D., Novák, P., Volný, M., and Havlícek, V. (2010) mMass 3: a cross-platform software environment for precise analysis of mass spectrometric data. *Anal. Chem.* **82,** 4648–4651